High-Frequency Acceleration: Therapeutic Tool to Preserve Bone following Tooth Extractions

M. Alikhani[1,2,3,4], J.A. Lopez[1,2], H. Alabdullah[1], T. Vongthongleur[1], C. Sangsuwon[1], M. Alikhani[1], S. Alansari[1,2], S.M. Oliveira[1,5], J.M. Nervina[1,2], and C.C. Teixeira[1,2,6]

Abstract

A common problem in clinical dentistry is the significant and rapid bone loss that occurs after tooth extraction. Currently there is no solution for the long-term preservation of alveolar bone. Previously, we showed that high-frequency acceleration (HFA) has an osteogenic effect on healthy alveolar bone. However, it is not known if HFA can preserve alveolar bone after extraction without negatively affecting wound healing. The purpose of this study was to evaluate the effect of HFA on alveolar bone loss and the rate of bone formation after tooth extraction. Eighty-five adult Sprague-Dawley rats were divided into 3 groups: control, static (static load), and HFA. In all groups, the maxillary right third molar was extracted. The HFA group received HFA for 5 min/d, applied through the second molar. The static group received the same magnitude of static load. The control group did not receive any stimulation. Some animals received fluorescent dyes at 26 and 54 d. Samples were collected on days 0, 7, 14, 28, and 56 for fluorescence microscopy, micro–computed tomography, histology, RNA, and protein analyses. We found that HFA increased bone volume in the extraction site and surrounding alveolar bone by 44% when compared with static, while fully preserving alveolar bone height and width long-term. These effects were accompanied by increased expression of osteogenic markers and intramembranous bone formation and by decreased expression of osteoclastic markers and bone resorption activity, as well as decreased expression of many inflammatory markers. HFA is a noninvasive safe treatment that can be used to prevent alveolar bone loss and/or accelerate bone healing after tooth extraction.

Keywords: bone formation, alveolar bone, socket healing, osteogenic response, mechanical stimulation, vibration

Introduction

Alveolar bone supports teeth; protects nerves, vessels, and glands; and supports muscles of mastication and facial expression. One common cause of alveolar bone loss is tooth extraction. Bone loss is greatest in the first 3 to 12 mo postextraction, with a loss of nearly 40% in height and 60% in width. This continues until only a narrow ridge remains or the alveolar bone is lost entirely. Approximately 50% of people aged 25 to 44 y and 70% of people aged 45 to 64 y have lost ≥1 teeth (excluding third molars), while 22% of people aged ≥75 y are completely edentulous (Dye et al. 2012; Slade et al. 2014). Therefore, alveolar bone loss negatively affects the oral health and quality of life for a significant portion of the US population (Trulsson et al. 2002; Emami et al. 2013).

The current options to preserve or improve postextraction alveolar bone dimensions are surgical bone grafts and guided bone regeneration (Bartee 2001; Wang and Lang 2012). Unfortunately, these procedures preserve bone height but not width (Ten Heggeler et al. 2011; Leblebicioglu et al. 2013). Additionally, bone grafting carries potential postoperative complications due to excessive inflammation or delayed healing (Morjaria et al. 2014), and cost may prevent some people from receiving these treatments. Thus, partially or fully edentulous patients are at risk for the devastating sequelae of alveolar bone loss, thus creating an urgent need for an affordable, conservative, and efficacious therapy that preserves alveolar bone long-term (Mardas et al. 2015; Willenbacher et al. 2015).

Mechanically stimulating teeth using high-frequency acceleration (HFA) induces alveolar bone formation in dentate rats

[1]Consortium for Translational Orthodontic Research, New York University College of Dentistry, New York, NY, USA
[2]Department of Orthodontics, New York University College of Dentistry, New York, NY, USA
[3]Department of Developmental Biology, Harvard School of Dental Medicine, Boston, MA, USA
[4]Department of Oral and Maxillofacial Surgery, New York University College of Dentistry, New York, NY, USA
[5]Department of Mechanical Engineering, Institute Polytechnic of Viseu, Viseu, Portugal
[6]Department of Basic Science and Craniofacial Biology, New York University College of Dentistry, New York, NY, USA

A supplemental appendix to this article is published electronically only at http://jdr.sagepub.com/supplemental.

Corresponding Author:
C.C. Teixeira, New York University, 345 East 24th Street, New York, NY 10010, USA.
Email: cristina.teixeira@nyu.edu

(Alikhani et al. 2012). HFA triggers skeletal adaptation to the altered levels and patterns of mechanical loading. It is unknown if HFA can simultaneously improve bone formation and decrease bone resorption in pathologic conditions, for example, during bone healing following tooth extraction. The objective of this investigation is to assess HFA as a noninvasive cost-effective treatment to maintain or improve alveolar bone after extractions.

Materials and Methods

Animal Study

The maxillary right third molar was extracted in 85 male Sprague-Dawley rats (400 g, 4 mo old) under intraperitoneal xylazine and ketamine-HCL anesthesia. Buprenorphine (analgesic) and Baytril (antibiotic) were given for 3 d postoperatively (protocol conforms to ARRIVE (Animal Research: Reporting of In Vivo Experiments) guidelines and was approved by New York University Institutional Animal Care and Use Committee). Rats were randomly divided into 3 groups. The HFA group received HFA (120 Hz, 0.3 g) applied to the occlusal surface of the maxillary right second molar for 5 min/d under 3% isoflurane anesthesia. This HFA regimen produced 4με (microstrain) in the surrounding bone. The static group received 4με of static load. The control group received no strain.

HFA and Static Force Application

Devices for HFA stimulation with low-magnitude force were prepared and calibrated at the mechanical engineering department of the Polytechnic Institute of Viseu–Portugal as described previously (Alikhani et al. 2012). Static load of 4με was delivered with the same device without activation (Appendix Fig. 1).

Micro–computed Tomography and Histomorphometry Analysis

Maxillae were scanned (μCT40; Scanco Medical, Bassersdorf, Switzerland), and histomorphometry data were generated with μCT V6.0 software on the HP open platform (OpenVMS Alpha Version 1.3-1 Session Manager). Bone fill was measured as bone volume/total volume (BV/TV) in defined boundaries on axial and sagittal slices through the entire volume of the right third molar extraction site (Fig. 1A). The boundaries were outlined on each axial slice as 2 lines parallel to the buccal and palatal bony plates (following the outline of the socket) and 2 parallel lines at the most mesial and distal points on the mesiobuccal and distobuccal roots, respectively. On each sagittal slice, the mesial and distal boundaries contacted the most mesial and distal points on the socket and were perpendicular to 2 reference lines: the incisal reference line ran through the furcation of the first and second molars; the apical reference line ran parallel to the incisal reference line along the most apical portion of the alveolus.

Micro–computed tomography quantification (Table) and alveolar bony changes were assessed in the region apical to the distal root. On each sagittal slice, a line was drawn at the most apical point of the distal root, perpendicular to the long axis of the root. A second line was drawn parallel to the first line, perpendicular to the long axis of the root, and tangent to the most apical point on the alveolus and the distance between these lines averaged (Fig. 2A). Alveolar height changes were evaluated on coronal slices through the extraction site. We averaged the greatest distance between the incisal and apical bone on the buccal and palatal plates to generate a single value for alveolar bone height on each slice (Fig. 2C).

Random and systematic errors were calculated according to Dahlberg and Houston (Da Souza Galvão et al. 2012). The random and systematic errors were found to be not significantly different for intraobserver (0.016 and 0.019 mm) and interobserver (0.020 and 0.024 mm) measurements.

Histology and Fluorescence Microscopy

Hemimaxillae were fixed in 4% paraformaldehyde, demineralized (14% EDTA for 2 wk), dehydrated in alcohol series, embedded in paraffin, and 5-μm slices cut. Five sections were immunostained (Vectastain ABC Kit; Vector Laboratories, Burlingame, CA, USA) with antibodies for tartarate-resistant acid phosphatase (TRAP; Zymed antibodies; Invitrogen, Carlsbad, CA, USA) to identify osteoclasts. As a negative control, sections were exposed to preimmune serum. Sections were scanned on a Scan Scope GL optical microscope (Aperio, Bristol, UK) at 20× magnification. Osteoclasts were defined as TRAP+ multinuclear cells on periosteal or endosteal surfaces from the distobuccal root of the maxillary second molar to the socket of third molar distobuccal root (apical and incisal reference lines described earlier). The number of TRAP+ cells per 1 mm^2 of alveolar bone was determined in 5 sections and averaged. Endochondral bone formation was assayed with toluidine blue staining of intermediate sections.

Rats received calcein (15 mg/kg, intraperitoneal) and xylenol orange (90 mg/kg, intraperitoneal) alternating on days 0, 28, and 54 and were euthanized on day 56. Hemimaxillae were fixed in formalin, washed overnight, dehydrated in alcohol, cleared in xylene, and embedded in methyl methacrylate (Erben 1997). Sections (7 to 10 μm thick; Leica RM2265 Microtome; Leica Biosystems, Buffalo Grove, IL, USA) were viewed by fluorescence microscopy (Nikon Microscopy; NIS-Elements Software, Tokyo, Japan) and photographed.

Quantitative Reverse Transcription Polymerase Chain Reaction Analysis

RNA was extracted from hemimaxillae ($n = 5$) on days 0, 3, and 14 as described previously (Oliveira et al. 2009). Inflammatory, osteogenic, and osteoclastic genes were analyzed with rat-specific primers via a QuantiTect SYBR Green RT-PCR Kit (Qiagen, Valencia, CA, USA) on a DNA Engine Optican 2 System (MJ Research, Waltham, MA, USA). Relative mRNA levels were calculated and normalized to

GAPDH and acidic ribosomal protein mRNA levels.

Protein Analysis

Total protein levels from hemimaxillae ($n = 5$) were quantitated with a BCA Protein Assay Kit (Pierce, Rockford, IL, USA). Enzyme-linked immunosorbent assay was used to measure activity of inflammatory markers (MyBiosource, San Diego, CA, USA) and a colorimetric assay used for alkaline phosphatase (Teixeira et al. 1995).
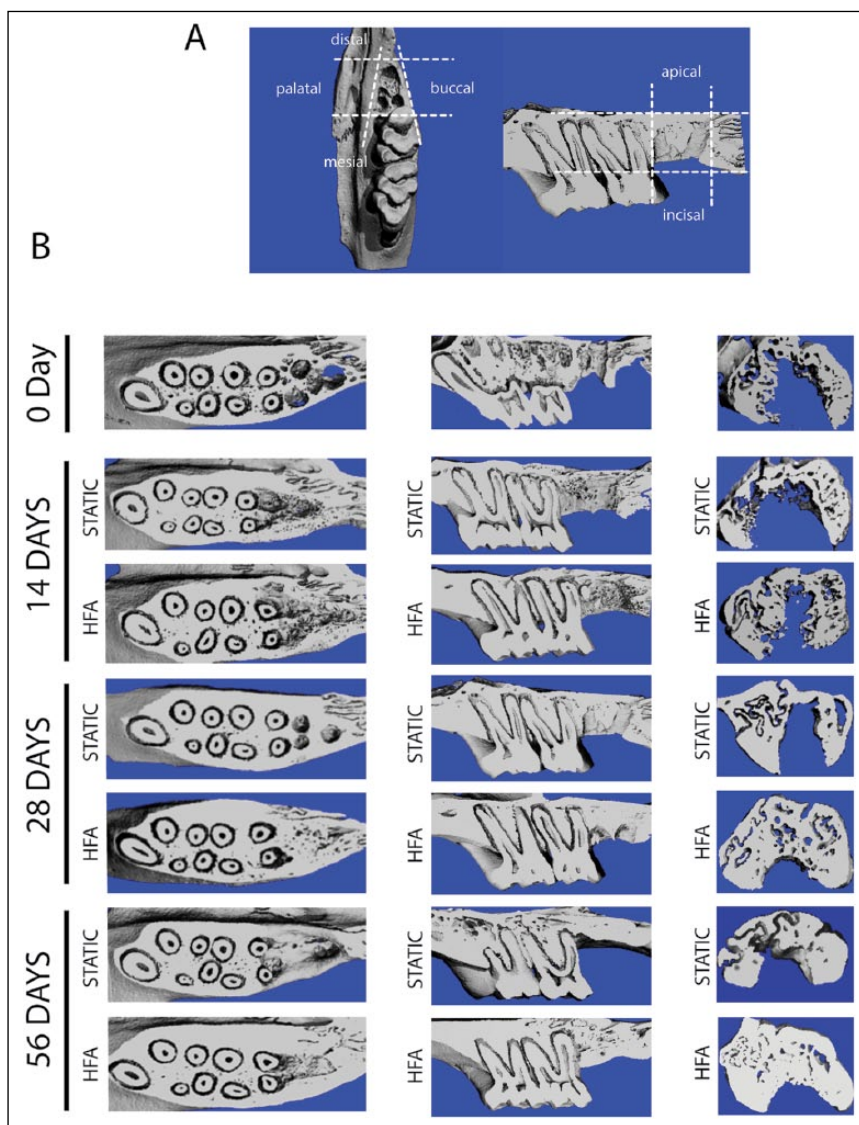
Statistics

Experiments were repeated at least 3 times. Data are reported as mean ± SEM. Significant differences between test groups and controls were assessed by analysis of variance. Pairwise multiple comparison analysis was performed by Tukey's post hoc test. Two-tailed P values were calculated, with statistical significance set at $P < 0.05$.

Results

HFA Accelerates Bone Healing in the Tooth Extraction Socket

Qualitative assessment of the third molar extraction site demonstrated marked increase in bone fill in the HFA group as compared with the baseline (day 0) and static group at day 28 and preservation of alveolar bone height at day 56 (Fig. 1B). Bone fill in the HFA and static groups was significantly different at day 14. To quantify the bone fill, BV/TV was compared in the extraction site among all groups (Table). The BV/TV in the area of the socket (Fig. 1A) increased from 27% (day 0) to 33%

Figure 1. High-frequency acceleration (HFA) stimulates alveolar bone formation in the extraction socket and surrounding alveolar bone. (**A**) Schematic of area/volume used for micro–computed tomography quantitative analysis, with dashed lines marking the borders in 3 planes of space. (**B**) Three-dimensional micro–computed tomography reconstructions show a higher level of bone formation and faster filling of alveolar socket in the area of the upper right third molar in the HFA samples in comparison with the static group at all time points after extraction. Occlusal view (furcation level), sagittal view (midsagittal section of alveolar ridge), and coronal view (distal root of right maxillary third molar) of the right hemimaxillae in both static and HFA groups after 0, 14, 28, and 56 d.

and 46% in static and HFA groups, respectively, 28 d after extraction. The differences between HFA and the other groups were statistically significant. No difference between static and control groups was detected (Appendix); therefore, for simplicity we present the data for static and HFA groups only.

Evaluation of the socket changes suggested that bone filling proceeded apically to cervically (Fig. 1B; compare 28-d sagittal and coronal slices for HFA and static groups). Indeed, at day 28, the HFA group versus the static group had significantly greater trabecular thickness, less trabecular spacing, and greater tissue mineral density in the bone of the apical third of the distal root (Table). We further examined the apical bone height (Fig. 2A) at days 0, 14, 28, and 56. At days 28 and 56 in

comparison with day 0, the static group had 1.4- and 2.6-fold increases, respectively, while the HFA group had 4.6- and 5.3-fold increases in height, respectively. No differences between static and control groups were observed (data not shown), and the difference between static and HFA groups at days 28 and 56 was statistically significant.

Application of HFA in the Long Term Preserves Alveolar Bone

At day 56, BV/TV in the extraction socket and surrounding area (Fig. 1A) was 18% and 62% for the static and HFA groups, respectively. In the bone of the apical third of the distal root,

Table. Micro–computed Tomography Analysis of Alveolar Bone.

Parameter	0 d	28 d		56 d	
		Static	HFA	Static	HFA
BV/TV, %	27.4 ± 3	33 ± 4.6	46 ± 5.9[a,b]	18 ± 4.8[a]	62 ± 7.2[a,b]
Tb.Th, mm	0.14 ± 0.02	0.16 ± 0.02	0.23 ± 0.01[a,b]	0.19 ± 0.02[a]	0.31 ± 0.01[a,b,c]
Tb.N, 1/mm	2.03 ± 0.24	2.06 ± 0.21	2 ± 0.20	2 ± 0.22	2.01 ± 0.21
Tb.Sp, mm	0.36 ± 0.05	0.33 ± 0.05	0.27 ± 0.04[a]	0.30 ± 0.01[a]	0.19 ±0.02[a,b,c]
TMD, mg/mL	396 ± 49	774 ± 46[a]	918 ± 68[a,b]	756 ± 54[a]	973 ± 52[a,b]

BV/TV, ratio of bone volume/total volume based on area defined in Figure 1A; HFA, high-frequency acceleration; Tb.N, trabecular number; Tb.Sp, trabecular spacing; Tb.Th, trabecular thickness; TMD, tissue mineral density.
Micro–computed tomography quantification was completed for static and HFA hemimaxillae at baseline (day 0) and 28 and 56 d after extraction. Tb.Th, Tb.N, Tb.Sp, and TMD were measured in the bone of the apical third of the socket of the distal root. Each value represents the mean ± SEM of 5 animals.
[a]Significantly different from day 0.
[b]Significantly different from static group at same time point
[c]Significantly different from same group at previous time point.
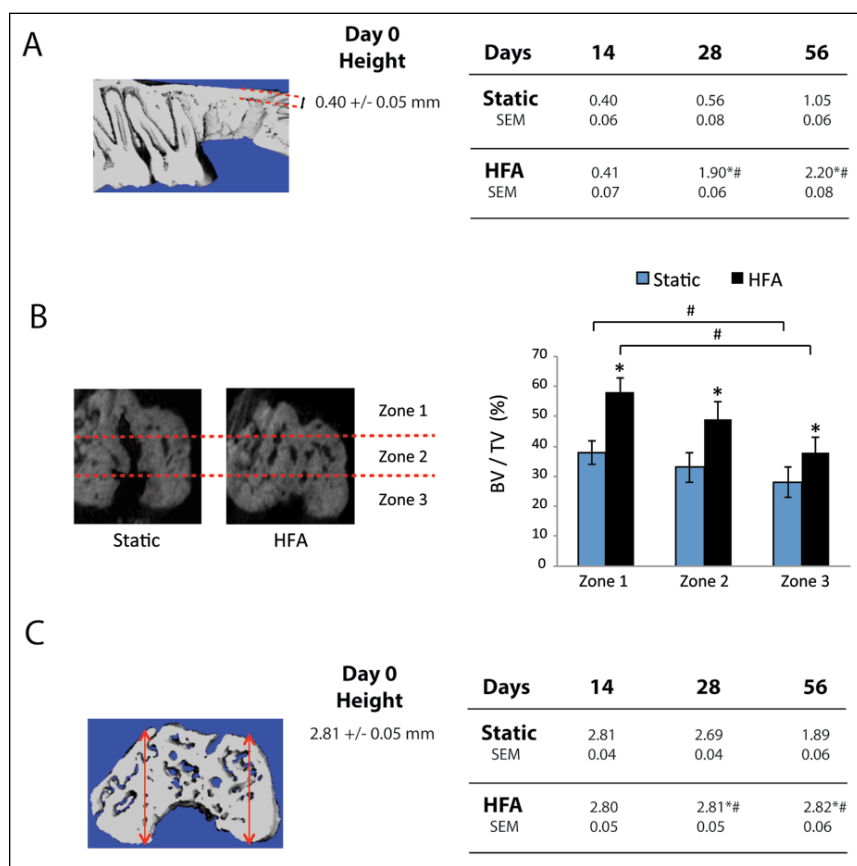
Figure 2. High-frequency acceleration (HFA) preserves alveolar bone height and increases bone volume in the extraction area. (**A**) Schematic of the midsagittal section of the alveolar ridge (between buccal and palatal cortical plate). This section was used for the measurement of bone height in the thinnest part of alveolar bone in the area of the distal root socket after extraction of upper right maxillary third molar. Each number represents the mean ± SEM collected from 5 animals. *Significantly different from baseline (day 0, shown in the middle). #Significantly different from static group at same time point. (**B**) Schematic of the area of analysis with zones identified in the micro–computed tomography section of the distal root of right maxillary third molar. Average bone volume fraction (bone volume/total volume [BV/TV]) was calculated for the apical (zone 1), middle (zone 2), and cervical thirds (zone 3) in both static and HFA groups after 56 d. Each value represents the mean ± SEM of 5 animals. *Significantly different from static group. #Significantly different from zone 1 for the same group. (**C**) Three-dimensional micro–computed tomography reconstructions of alveolar socket in area of distal root of upper right third molar at 0, 14, 28, and

the trabecular thickness was 63% greater, trabecular spacing 37% less, and bone mineral density 28% greater in the HFA group versus the static group (Table). The differences between HFA and the other groups were statistically significant for all parameters studied except trabecular number. Confirming the enhanced apical bone response and showing long-term preservation of alveolar bone, we found that coronal sections at day 56 (Fig. 2B) showed 58%, 49%, and 38% BV/TV in apical (zone 1), middle (zone 2), and cervical (zone 3) regions, respectively, of the HFA group, which were statistically different from the corresponding regions in the static group (38%, 33%, and 28%, respectively). Moreover, the apical region showed significantly greater BV/TV than the cervical region for both HFA and static groups.

HFA also significantly increased and preserved alveolar bone height over the long term when compared with the static group at days 28 and 56 (Fig. 1C). When quantitated, alveolar bone height was significantly greater in the HFA group versus the static group at both times (Fig. 2C). Comparing days 28 and

56 d. Buccal and palatal cortical plate height was measured in 3 sections of alveolar ridge in the area of extraction (mesial, middle, and distal). Each number represents the mean ± SEM of measurements from 5 animals. *Significantly different from baseline (day 0, shown in the middle). #Significantly different from static group at same time point.
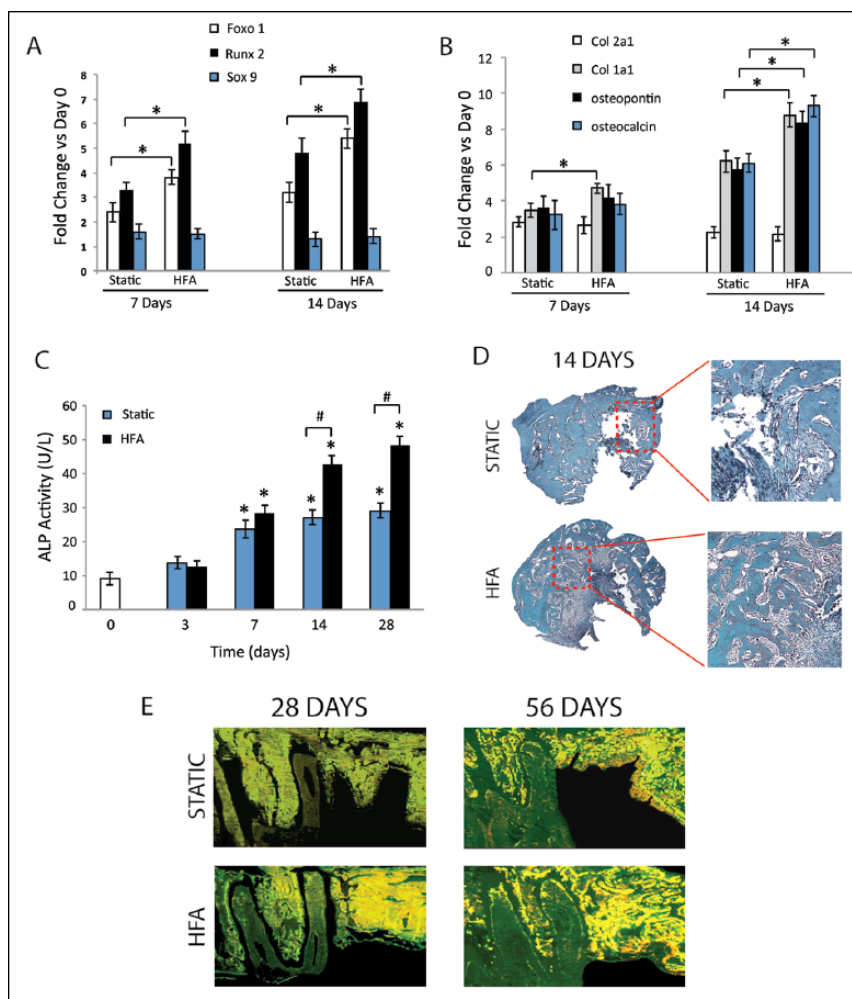
56 with day 0, the static group lost 4% and 52.9% of their alveolar bone height, respectively, while alveolar bone in the HFA group remained unchanged. No difference between static and control group was observed (data not shown). Importantly, the differences between static and HFA groups at days 28 and 56 were statistically significant and were due entirely to alveolar bone loss in the static group.

HFA Increases Bone Healing through Intramembranous Ossification

To investigate whether HFA accelerates bone healing through endochondral or intramembranous bone formation, expression of osteoblastic and chondrogenic markers in alveolar bone in and around the extraction site were studied at days 7 and 14. Expression of Foxo1, Runx2, and Sox9, which are critical determinants of intramembranous versus endochondral bone formation (de Crombrugghe et al. 2000; de Crombrugghe et al. 2001; Teixeira et al. 2010), increased significantly at both days (Fig. 3A). At day 7, Foxo1 and Runx2 mRNA levels increased 3.8- and 5.2-fold, respectively, in HFA, as compared with 2.4- and 3.3-fold increases, respectively, in the static group. At day 14, Foxo1 and Runx2 mRNA levels increased 5.4- and 6.9-fold in the HFA group and 3.2- and 4.8-fold in the static group, respectively. Sox9 mRNA did not change significantly in either group.

Col1a1 mRNA levels increased significantly at days 7 (4.7-fold) and 14 (8.8-fold) in the HFA group when compared with the static group (3.5- and 6.2-fold, respectively; Fig. 3B). Col2a1

Figure 3. High-frequency acceleration (HFA) stimulates intramembranous bone formation. RNA was collected from baseline (day 0) and static and HFA groups at days 7 and 14 after extraction of upper right maxillary third molar, and the expression of different transcription factors (**A**) and osteogenic and chondrogenic factors (**B**) were evaluated by reverse transcription polymerase chain reaction. Data shown as fold change in comparison to day 0. Except for Sox9 expression, all data presented are significantly different from day 0. *Significantly different from static group at same time point. (**C**) Cell extract was also collected from different samples for analysis of alkaline phosphatase (ALP) activity at days 0, 3, 7, 14, and 28. *Significantly different from day 0. #Significantly different from static group at same time point. (**D**) Histologic staining for cartilage at day 14 for both static and HFA groups (toluidine blue staining) demonstrate absence of cartilage during socket healing in both groups. (**E**) Fluorescence microscopy of sagittal sections at days 28 and 56 shows increased intensity of the labels in extraction area of HFA samples indicative of extensive bone formation.

mRNA levels increased in both static and HFA groups, but no difference between the groups was observed. Osteopontin (8.4-fold) and osteocalcin (9.3-fold) mRNA levels were significantly higher in the HFA group than the static group only at day 14 (5.8- and 6.1-fold, respectively). No difference between the static and control groups was observed (data not shown).

Both static and control groups demonstrated significantly higher alkaline phosphatase (ALP) activity at day 7 compared with baseline (day 0), but no difference between the groups was observed at day 3 and day 7 (Fig. 3C). The HFA group exhibited significantly higher ALP activity at days 14 (54%) and 28 (65%) compared with the static group.

To investigate endochondral bone formation during postextraction healing, day 14 histologic sections were stained with toluidine blue to identify cartilage in the HFA and static groups (Fig. 3D). In both groups, only woven bone formation was observed extending from the old bone of the socket walls toward the center of the socket. No cartilage formation was observed in either group.

Fluorescence microscopy revealed marked bone formation activity and bone fill at the extraction site at day 28 in the HFA group compared with the static group (Fig. 3E). At day 56 significantly higher bone formation activity was observed in the HFA group, with bone completely filling the extraction site and
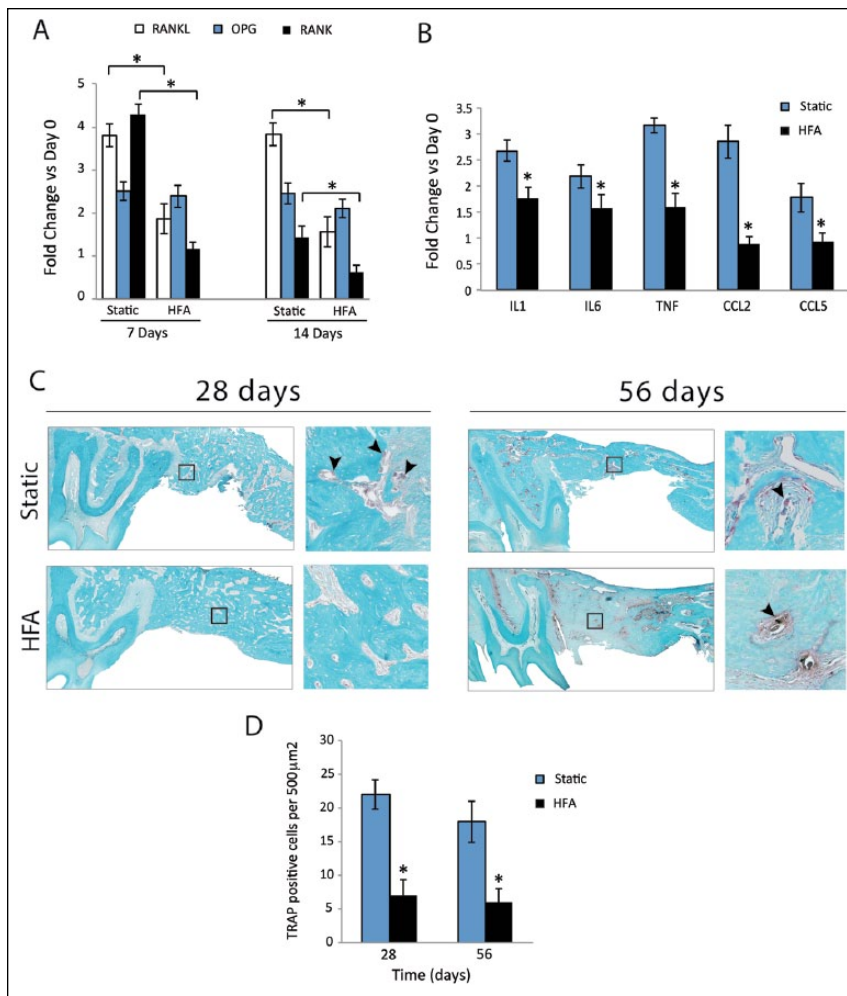
Figure 4. High-frequency acceleration (HFA) inhibits bone resorption after tooth extraction. RNA was collected from the right hemimaxillae of baseline (day 0) and static and HFA animals at days 7 and 14, and the expression of different regulators of osteoclastogenesis genes (**A**) and inflammatory genes (day 7; **B**) was evaluated by reverse transcription polymerase chain reaction. Data shown as fold change in comparison to day 0. HFA reduces the expression of genes that participate in osteoclastogenesis and inflammation. (**C**) TRAP (tartarate-resistant acid phosphatase) staining of right hemimaxillae after 28 and 56 d. Sagittal sections of right maxilla were produced through the roots of second molar in static and HFA samples. TRAP staining sections shown with magnified detail of marked square area. At 28 d, sections demonstrate higher number of osteoclasts (arrowheads) in the static group than in the HFA group. At 56 d, lamellar bone gradually replaces the woven bone, while the static group still demonstrates higher number of osteoclasts. (**D**) Mean numbers of osteoclasts at 28 and 56 d in extraction area. Each value represents the mean ± SEM of 5 animals. *Significantly different from static group at similar time points.

additional bone being deposited (orange labeling) throughout the socket.

HFA Decreases Expression of Osteoclastogenesis Markers and Osteoclast Number

The expression of osteoclastogenesis regulators was studied in and around the extraction site. At day 14, the HFA group showed 52% and 73% decreased RANKL and RANK mRNA levels, respectively, compared with the static group. Likewise, at day 28 RANKL and RANK mRNA levels were 60% and 57% lower in the HFA and static groups, respectively (Fig.

4A). No significant difference in osteoprotegerin (OPG) mRNA levels between groups at days 14 or 28 was observed.

Inflammatory cytokines are upstream regulators of osteoclast differentiation and activation and may play a role in skeletal wound healing (Galliera et al. 2012). At day 14, the HFA group demonstrated significantly lower IL-1 (35%), IL-6 (28%), TNF-α (48%), CCL2 (69%), and CCL5 (48%) expression when compared with the static group (Fig. 4B).

Histologically, the number of TRAP+ cells in the static group increased significantly when compared with the HFA group at day 28 (Figs. 4C, D). At day 56, the number of TRAP+ cells remained high in the static group and low in the HFA group (Fig. 4D) as lamellar bone replaced woven bone.

Discussion

Tooth loss leads invariably to progressive irreversible alveolar bone atrophy due to varying combinations of jaw anatomy, age, sex, hormonal changes, local inflammation, and masticatory habits (Kingsmill 1999; Clementini et al. 2014). Another key contributor to postextraction alveolar bone resorption is loss of masticatory forces transmitted through tooth roots to the surrounding alveolar bone (Ulm et al. 1997). Logically, restoring mechanical stimulation around the extraction site should preserve postextraction alveolar bone. We demonstrated here one approach to providing this treatment.

The major obstacle in developing a mechanical treatment that preserves postextraction alveolar bone is delivering enough osteogenic strain (0.1%) to produce sufficient matrix deformation (Frost 1987; Turner et al. 1994) without fracturing the fragile alveolar bone. Interestingly, applying low strain (<0.001%) at high frequency produces osteogenic matrix deformation in weight-bearing bones (Rubin et al. 2001; Oxlund et al. 2003). Fortunately, osteogenic strain can also be manipulated by varying the strain magnitude (Rubin and Lanyon 1984), strain rate (O'Connor et al. 1982), electrokinetic streaming currents (Pollack et al. 1984), piezoelectric currents (Bassett 1968), fluid shear flow (Weinbaum et al. 1994), or strain energy density (Aguado et al. 2015).

The mechanism by which low strain is osteogenic is unknown. The probability that matrix deformation (or its

by-products—e.g., streaming potentials, fluid drag, enhanced nutrient transport; Qin et al. 2003; Malone et al. 2007) is the sole contributor to strain-induced osteogenesis is unlikely because matrix deformation at low strain is too small to be detected by cells. This suggests that mechanical stimulation may produce other important osteogenic signals. Physical acceleration of a cell may be such a signal (Garman et al. 2007).

Bone, cartilage, and ligament cells respond to markedly different ranges of strain, yet the resulting cellular accelerations fall within a narrow range. It should be emphasized that higher accelerations usually require higher strains, which sets limits on the osteogenic response if acceleration is the only treatment being considered. However, manipulating acceleration frequency is a safe compensation for this shortcoming. Indeed, HFA application, independent of matrix deformation, enhances bone formation in weight-bearing bones (Garman et al. 2007) and increases bone-healing rates (Omar et al. 2008; Goodship et al. 2009). Likewise, we significantly increase osteogenesis in alveolar bone using HFA with almost no matrix deformation (Alikhani et al. 2012).

Interestingly, HFA's osteogenic effect on alveolar bone extends beyond the point of HFA application (Alikhani et al. 2012). Our finding that HFA applied to the second molar significantly improved bone fill in the third molar socket confirms this phenomenon. This is clinically significant because it verifies that HFA can safely increase bone formation in fragile areas such as extraction sites. While the gradient boundaries of HFA's osteogenic effect remain to be determined, we predict that alveolar bone density will produce a relatively tight gradient. Delineating the HFA's "reach" is important for clinicians who must carefully consider unwanted side effects on adjacent teeth or delicate mucosa when designing devices and applying HFA treatments.

Some studies have shown the expression of cartilage-specific genes during bone healing of extraction sockets (Ting et al. 1993; Shyng et al. 1999). Because bone and cartilage cells can respond to mechanical stimulation, we decided to evaluate both intramembranous and endochondral pathways in the healing process in response to HFA. Mechanistically, our results suggest that HFA primarily induced intramembranous bone formation. This is in spite of increased Col2a1 expression in both control and HFA groups. Col2a1 is the primary extracellular matrix protein in cartilage, is highly expressed during endochondral bone healing, and is expressed at early stages of mesenchymal stem cell differentiation before commitment to the intramembranous pathway (Miljkovic et al. 2008; Palomares et al. 2009). Increased Foxo1 activation in early stages of socket healing also demonstrates commitment of these cells toward the osteogenic pathway (Teixeira et al. 2010).

While it is clear that HFA promotes skeletal wound healing, the molecular and physical mechanisms regulating this are not clear. It has been suggested that oscillating nuclei activate the cytoskeleton, which then increases osteoblast activity. Indeed, osteoblast markers (Col1a1, osteopontin, and osteocalcin) all increased significantly in our HFA-treated animals. This is in agreement with previous work demonstrating HFA's osteogenic effect in weight-bearing bones (Rubin et al. 2001). These data support the conclusion that HFA directly promotes molecular and physical responses in osteoblast during wound healing.

Interestingly, HFA also decreased RANKL expression and the number of osteoclasts. The antiresorptive effect of high-frequency, low-magnitude forces has been ascribed to osteocyte activation and release of TGF-β, nitric oxide, and prostaglandins that decrease osteoclast formation (Lau et al. 2010). We also found decreased inflammatory marker expression suggesting that HFA affects all local cells (inflammatory and noninflammatory cells, including osteocytes), which can decrease RANKL expression and osteoclast activation. Since HFA did not affect OPG expression significantly, our results suggest that the decrease in RANKL, rather than OPG competition, is the primary reason why osteoclast numbers declined following HFA treatment.

Our study supports HFA as a simple treatment to promote alveolar bone formation. Applying HFA for just 5 min/d as part of a home care regimen may significantly improve outcomes of procedures such as tooth extraction, implant and bone graft integration, and postorthodontic retention, as well as diseases such as osteoporosis and periodontal disease. Further research in this field will help uncover the mechanism of skeletal adaptation to mechanical stimulation and how to manipulate HFA to treat bone loss and injuries in non-weight-bearing bones.

Author Contributions

M. Alikhani, C.C. Teixeira, contributed to conception, design, and data analysis, drafted and critically revised the manuscript; J.A. Lopez, H. Alabdullah, C. Sangsuwon, M. Alikhani, S.M. Oliveira, contributed to conception, design, and data acquisition, critically revised the manuscript; T. Vongthongleur, contributed to data acquisition, critically revised the manuscript; S. Alansari, contributed to conception, design, data acquisition, and analysis, drafted and critically revised the manuscript; J.M. Nervina, contributed to data analysis, drafted and critically revised the manuscript. All authors gave final approval and agree to be accountable for all aspects of the work.

Acknowledgments

References

Aguado E, Pascaretti-Grizon F, Goyenvalle E, Audran M, Chappard D. 2015. Bone mass and bone quality are altered by hypoactivity in the chicken. PLoS One. 10(1):e0116763.

Alikhani M, Khoo E, Alyami B, Raptis M, Salgueiro JM, Oliveira SM, Boskey A, Teixeira CC. 2012. Osteogenic effect of high-frequency acceleration on alveolar bone. J Dent Res. 91(4):413–419.

Bartee BK. 2001. Extraction site reconstruction for alveolar ridge preservation: part 2. Membrane-assisted surgical technique. J Oral Implantol. 27(4):194–197.

Bassett CA. 1968. Biologic significance of piezoelectricity. Calcif Tissue Res. 1(4):252–272.

Clementini M, Rossetti PH, Penarrocha D, Micarelli C, Bonachela WC, Canullo L. 2014. Systemic risk factors for peri-implant bone loss: a systematic review and meta-analysis. Int J Oral Maxillofac Surg. 43(3):323–334.

Da Souza Galvão MC, Sato JR, Coelho EC. 2012. Dahlberg formula: a novel approach for its evaluation. Dental Press J Orthod. 17(1)115–124.

de Crombrugghe B, Lefebvre V, Behringer RR, Bi W, Murakami S, Huang W. 2000. Transcriptional mechanisms of chondrocyte differentiation. Matrix Biol. 19(5):389–394.

de Crombrugghe B, Lefebvre V, Nakashima K. 2001. Regulatory mechanisms in the pathways of cartilage and bone formation. Curr Opin Cell Biol. 13(6):721–727.

Dye BA, Li X, Thorton-Evans G. 2012. Oral health disparities as determined by selected healthy people 2020 oral health objectives for the United States, 2009–2010. NCHS Data Brief. 2012(104):1–8.

Emami E, De Souza RF, Kabawat M, Feine JS. 2013. The impact of edentulism on oral and general health. Int J Dent. 2013:2013498305.

Erben RG. 1997. Embedding of bone samples in methylmethacrylate: an improved method suitable for bone histomorphometry, histochemistry, and immunohistochemistry. J Histochem Cytochem. 45(2):307–313.

Frost HM. 1987. The mechanostat: a proposed pathogenic mechanism of osteoporoses and the bone mass effects of mechanical and nonmechanical agents. Bone Miner. 2(2):73–85.

Galliera E, Corsi MM, Banfi G. 2012. Platelet rich plasma therapy: inflammatory molecules involved in tissue healing. J Biol Regul Homeost Agents. 26(2 Suppl 1):35S-42S.

Garman R, Rubin C, Judex S. 2007. Small oscillatory accelerations, independent of matrix deformations, increase osteoblast activity and enhance bone morphology. PLoS One. 2(7):e653.

Goodship AE, Lawes TJ, Rubin CT. 2009. Low-magnitude high-frequency mechanical signals accelerate and augment endochondral bone repair: preliminary evidence of efficacy. J Orthop Res. 27(7):922–930.

Kingsmill VJ. 1999. Post-extraction remodeling of the adult mandible. Crit Rev Oral Biol Med. 10(3):384–404.

Lau E, Al-Dujaili S, Guenther A, Liu D, Wang L, You L. 2010. Effect of low-magnitude, high-frequency vibration on osteocytes in the regulation of osteoclasts. Bone. 46(6):1508–1515.

Leblebicioglu B, Salas M, Ort Y, Johnson A, Yildiz VO, Kim DG, Agarwal S, Tatakis DN. 2013. Determinants of alveolar ridge preservation differ by anatomic location. J Clin Periodontol. 40(4):387–395.

Malone AM, Batra NN, Shivaram G, Kwon RY, You L, Kim CH, Rodriguez J, Jair K, Jacobs CR. 2007. The role of actin cytoskeleton in oscillatory fluid flow-induced signaling in MC3T3–E1 osteoblasts. Am J Physiol Cell Physiol. 292(5):C1830–C1836.

Mardas N, Trullenque-Eriksson A, Macbeth N, Petrie A, Donos N. 2015. Does ridge preservation following tooth extraction improve implant treatment outcomes: a systematic review: Group 4: Therapeutic concepts & methods. Clin Oral Implants Res. 26 Suppl 11:180–201.

Miljkovic ND, Cooper GM, Marra KG. 2008. Chondrogenesis, bone morphogenetic protein-4 and mesenchymal stem cells. Osteoarthritis Cartilage. 16(10):1121–1130.

Morjaria KR, Wilson R, Palmer RM. 2014. Bone healing after tooth extraction with or without an intervention: a systematic review of randomized controlled trials. Clin Implant Dent Relat Res. 16(1):1–20.

O'Connor JA, Lanyon LE, MacFie H. 1982. The influence of strain rate on adaptive bone remodelling. J Biomech. 15(10):767–781.

Oliveira NF, Damm GR, Andia DC, Salmon C, Nociti FH Jr, Line SR, De Souza AP. 2009. DNA methylation status of the IL8 gene promoter in oral cells of smokers and non-smokers with chronic periodontitis. J Clin Periodontol. 36(9):719–725.

Omar H, Shen G, Jones AS, Zoellner H, Petocz P, Darendeliler MA. 2008. Effect of low magnitude and high frequency mechanical stimuli on defects healing in cranial bones. J Oral Maxillofac Surg. 66(6):1104–1111.

Oxlund BS, Ørtoft G, Andreassen TT, Oxlund H. 2003. Low-intensity, high-frequency vibration appears to prevent the decrease in strength of the femur and tibia associated with ovariectomy of adult rats. Bone. 32(1):69–77.

Palomares KT, Gleason RE, Mason ZD, Cullinane DM, Einhorn TA, Gerstenfeld LC, Morgan EF. 2009. Mechanical stimulation alters tissue differentiation and molecular expression during bone healing. J Orthop Res. 27(9):1123–1132.

Pollack SR, Petrov N, Salzstein R, Brankov G, Blagoeva R. 1984. An anatomical model for streaming potentials in osteons. J Biomech. 17(8): 627–636.

Qin J, Kang W, Leung B, Mcleod M. 2003. Ste11p, a high-mobility-group box DNA-binding protein, undergoes pheromone- and nutrient-regulated nuclear-cytoplasmic shuttling. Mol Cell Biol. 23(9):3253–3264.

Rubin CT, Lanyon LE. 1984. Regulation of bone formation by applied dynamic loads. J Bone Joint Surg Am. 66(3):397–402.

Rubin CT, Sommerfeldt DW, Judex S, Qin Y. 2001. Inhibition of osteopenia by low magnitude, high-frequency mechanical stimuli. Drug Discov Today. 6(16):848–858.

Shyng YC, Devlin H, Riccardi D, Sloan P. 1999. Expression of cartilage-derived retinoic acid-sensitive protein during healing of the rat tooth-extraction socket. Arch Oral Biol. 44(9):751–757.

Slade GD, Akinkugbe AA, Sanders AE. 2014. Projections of U.S. edentulism prevalence following 5 decades of decline. J Dent Res. 93(10):959–965.

Teixeira CC, Hatori M, Leboy PS, Pacifici M, Shapiro IM. 1995. A rapid and ultrasensitive method for measurement of DNA, calcium and protein content, and alkaline phosphatase activity of chondrocyte cultures. Calcif Tissue Int. 56(3):252–256.

Teixeira CC, Liu Y, Thant LM, Pang J, Palmer G, Alikhani M. 2010. Foxo1, a novel regulator of osteoblast differentiation and skeletogenesis. J Biol Chem. 285(40):31055–31065.

Ten Heggeler JM, Slot DE, Van Der Weijden GA. 2011. Effect of socket preservation therapies following tooth extraction in non-molar regions in humans: a systematic review. Clin Oral Implants Res. 22(8):779–788.

Ting K, Petropulos LA, Iwatsuki M, Nishimura I. 1993. Altered cartilage phenotype expressed during intramembranous bone formation. J Bone Miner Res. 8(11):1377–1387.

Trulsson U, Engstrand P, Berggren U, Nannmark U, Branemark PI. 2002. Edentulousness and oral rehabilitation: experiences from the patients' perspective. Eur J Oral Sci. 110(6):417–424.

Turner CH, Forwood MR, Rho JY, Yoshikawa T. 1994. Mechanical loading thresholds for lamellar and woven bone formation. J Bone Miner Res. 9(1):87–97.

Ulm CW, Kneissel M, Hahn M, Solar P, Matejka M, Donath K. 1997. Characteristics of the cancellous bone of edentulous mandibles. Clin Oral Implants Res. 8(2):125–130.

Wang RE, Lang NP. 2012. Ridge preservation after tooth extraction. Clin Oral Implants Res. 23 Suppl 6:147–156.

Weinbaum S, Cowin SC, Zeng Y. 1994. A model for the excitation of osteocytes by mechanical loading-induced bone fluid shear stresses. J Biomech. 27(3):339–360.

Willenbacher M, Al-Nawas B, Berres M, Kammerer PW, Schiegnitz E. 2015. The effects of alveolar ridge preservation: a meta-analysis. Clin Implant Dent Relat Res [epub ahead of print 1 Jul 2015] in press. doi:10.1111/cid.12364